JCTC Journal of Chemical Theory and Computation

pubs.acs.org/JCTC Letter

Large Scale Quantum Chemistry with Tensor Processing Units

Ryan Pederson,* John Kozlowski, Ruyi Song, Jackson Beall, Martin Ganahl, Markus Hauru, Adam G. M. Lewis, Yi Yao, Shrestha Basu Mallick, Volker Blum, and Guifre Vidal

Cite This: *J. Chem. Theory Comput.* 2023, 19, 25−32 Read Online

ACCESS | Metrics & More | Article Recommendations | Supporting Information

ABSTRACT: We demonstrate the use of Googles cloud-based Tensor Processing Units (TPUs) to accelerate and scale up conventional (cubic-scaling) density functional theory (DFT) calculations. Utilizing 512 TPU cores, we accomplish the largest such DFT computation to date, with 247848 orbitals, corresponding to a cluster of 10327 water molecules with 103270 electrons, all treated explicitly. Our work thus paves the way toward accessible and systematic use of conventional DFT, free of any system-specific constraints, at unprecedented scales.

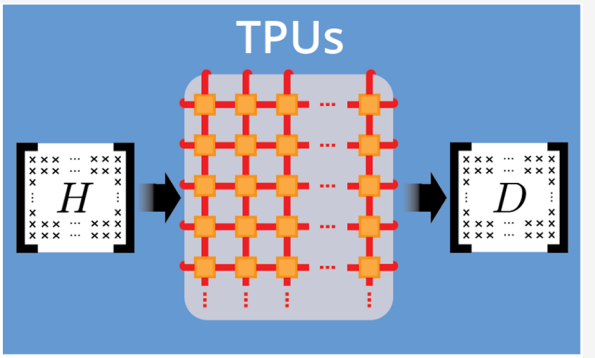

INTRODUCTION

Computational methods for quantum chemistry and quantum physics have proven to be invaluable tools in modern scientific research and technological innovation. The application space of such methods is vast, ranging from the prediction of novel high-temperature superconductors[1] to the acceleration of drug discovery[2] and from the study of catalytic processes for e.g. CO_2 sequestration[3] and plastic recycling[4] to the design of nanomaterials,[5] solar cells,[6] and batteries.[7]

In the landscape of quantum-based computational methods, density functional theory (DFT) especially stands out due to its ability to produce accurate results for a wide range of systems at a relatively low computational cost.[8] Accordingly, an impressive amount of computational research utilizes DFT calculations each year. For instance, the US National Energy Research Scientific Computing Center (NERSC) reported that nearly 30% of their supercomputer resources in 2018 were spent on DFT calculations alone.[9] Widespread research and development efforts are continuously devoted toward optimizing the performance and accuracy of DFT calculations, giving rise to a plethora of open-source and commercial DFT software packages.[10] Several packages can leverage specialized hardware, such as general-purpose graphics processing units (GPUs), for most of the workload.[11−17] However, in conventional DFT implementations, i.e., without specific sparsity assumptions for the density matrix or Hamiltonian matrix, the computational cost scales as the third power of the number N of orbitals used to describe the system (referred to as $O(N^3)$ DFT throughout this work), and this cubic scaling often makes simulating large systems, such as protein−ligand complexes or metal−organic frameworks,[18] prohibitively expensive.

Google's Tensor Processing Units (TPUs) are application-specific integrated circuits originally designed to accelerate large-scale machine learning workloads.[19−23] By leveraging the JAX library,[21−23] it is nevertheless possible to repurpose TPUs for other computational tasks.[24−35] In this work, we demonstrate the use of TPUs as quantum chemistry supercomputers by accelerating the $O(N^3)$ computational bottleneck of DFT approaches which use an auxiliary single-particle kinetic energy approximation, such as Kohn−Sham (KS)[36,37] and generalized KS (gKS)[38] DFT, where gKS admits hybrid DFT functionals. This enables the systematic study of quantum chemistry problems at unprecedented scales. As a concrete demonstration, we performed end-to-end $O(N^3)$ DFT calculations on large clusters of water molecules, reaching a total of N = 247 848 DFT orbitals, corresponding to 10 327 water molecules with 103 270 electrons, see Figure 1 and Table 1. To our knowledge, this is the largest $O(N^3)$ DFT calculation to date, with the previously largest computation consisting of a single $O(N^3)$ DFT iteration with $N \approx$ 230 000 orbitals on Fujitsu's K computer.[39]

Some variants of DFT, most notably linear-scaling DFT,[40−43] avoid the $O(N^3)$ bottleneck altogether and can thus reach an even larger number of orbitals. However, these variants rely on additional approximations and conditions, such

Received: August 25, 2022
Published: December 12, 2022

https://doi.org/10.1021/acs.jctc.2c00876
J. Chem. Theory Comput. 2023, 19, 25−32

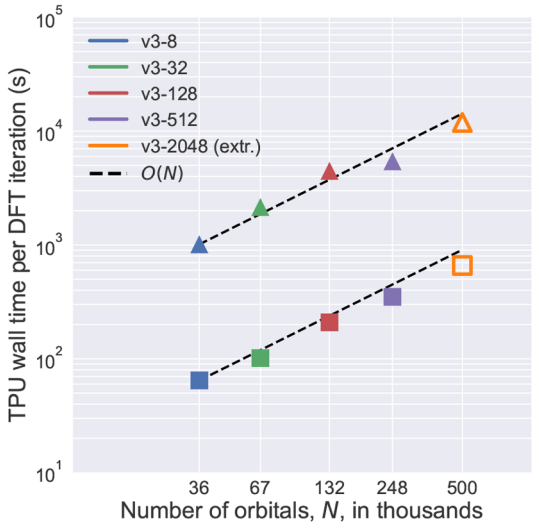

Figure 1. TPU v3 wall time for $O(N^3)$ density matrix purification, eqs 5-7, as a function of the number N of orbitals, for clusters of water molecules, both in single (squares) and double (triangles) precision. A full TPU v3 pod with 2048 cores and 32 TB of memory is expected to handle $N \sim 500\,000$ orbitals in our current implementation (extrapolated results necessitated by temporary resource unavailability).

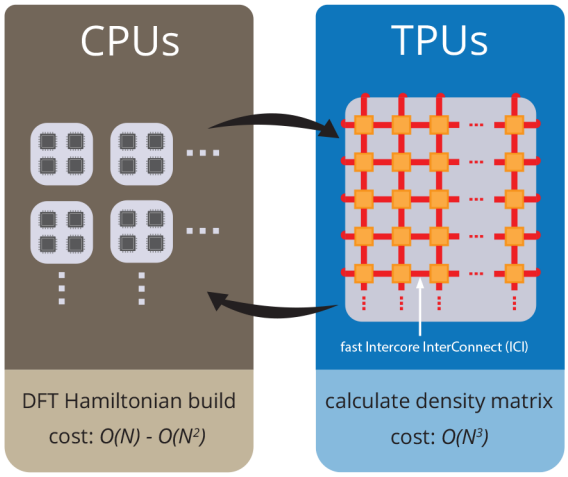

Figure 2. Two main steps of our implementation of an $O(N^3)$ DFT computation, the Hamiltonian build and computing the ground state density matrix, which we run on CPUs and TPUs, respectively. The DFT code FHI-aims[46,47] is used to set up the Hamiltonian, and the ELSI library[48,49] is used to facilitate the integration of the TPU-based solver to FHI-aims.

as truncating density matrix elements,[44] or on special properties of only a subset of density functionals (such as semilocal density functional approximations). In turn, this results in restricted applicability, with e.g. linear-scaling DFT being suitable for insulating systems but not for metals or systems with a small energy gap.[40] In practice, conventional $O(N^3)$ DFT is a more preferable choice since it alleviates technical complexity and problem space restrictions associated with current lower-scaling methods, greatly extending the domain of problems to which DFT can be applied reliably and with relative ease.

There are many aspects that go into an $O(N^3)$ DFT calculation. Throughout, we focus on atom-centered basis sets with all electrons treated explicitly, that is we do not consider e.g. plane waves or pseudopotentials. At a high level, one can identify two main computational steps: (a) building the DFT Hamiltonian matrix (with cost $O(N)$ to $O(N^2)$) and (b) computing the ground state density matrix ($O(N^3)$), see Figure 2.

(a) *DFT Hamiltonian build*: Given a choice of N atom-centered basis functions $\chi_i(\mathbf{r})$, one needs to compute the DFT Hamiltonian matrix H and the overlap matrix S, with coefficients given by

$$H_{ij} = \langle \chi_i | \mathcal{H} | \chi_j \rangle, \quad S_{ij} = \langle \chi_i | \chi_j \rangle \tag{1}$$

where $\mathcal{H}$ represents the DFT Hamiltonian in the continuum, and each matrix coefficient requires computing one or several integrals. Over the past few decades, much effort has been devoted to optimizing the build of the $N \times N$ matrix H. Naively, the computational time here scales as $O(N^4)$; however, in many implementations, the scaling is effectively reduced to $O(N^2)$ due to two-electron integral screening methods. The scaling can be further reduced to almost $O(N)$ if other strategies, such as fast multipole methods[45] or fast Fourier transform based methods,[43] such as the Ewald method for periodic systems, are employed. In this work, we do *not* attempt to accelerate the Hamiltonian or overlap matrix build times with TPUs. Instead, we simply use a well-established all-electron DFT package, the *Fritz Haber Institute ab initio molecular simulations package* (FHI-aims),[11,46,47] which we run using CPUs.

(b) *Density matrix purification:* The pair of matrices H and S defines a generalized eigenvalue problem, the so-called KS equations

$$H|\phi_\alpha\rangle = e_\alpha S|\phi_\alpha\rangle \tag{2}$$

where $|\phi_\alpha$ and e_α are the KS orbitals and energies. Our goal is to compute the ground state density matrix

Table 1. Tabulated Results in Figure 1, Including Also the Number of Atoms and Electrons[a]

				TPU wall time (s)		
no. of orbitals	no. of atoms	no. of electrons	TPU configuration	FP32	FP64	relative energy per molecule (mHa)
35 544	4 443	14 810	v3-8	65	1 012	0.934
65 668	8 211	27 370	v3-32	102	2 150	0.531
131 544	16 443	54 810	v3-128	209	4 465	0.291
247 848	30 981	103 270	v3-512	350	5 434	0

[a]Wall times for the matrix purification step are shown both for single (FP32) and double (FP64) precision. Energies are relative to the largest calculation, $E[(H_2O)_{N_{mol}}]/N_{mol} - E[(H_2O)_{10327}]/10327$, where N_{mol} is the total number of water molecules. In this sequence, we used a number of TPU cores that grow roughly as N^2. As a result, walltimes are seen to roughly scale linearly in N, instead of the expected $O(N^3)$ scaling.

https://doi.org/10.1021/acs.jctc.2c00876
J. Chem. Theory Comput. 2023, 19, 25−32

$$D \equiv \sum_{\alpha=1}^{N} \theta(\mu - e_\alpha)|\phi_\alpha\rangle\langle\phi_\alpha| \tag{3}$$

where $\theta(x)$ is the step function, and μ is the chemical potential, chosen such that $\sum_{\alpha=1}^{N}\theta(\mu-e_\alpha) = N_e$, where N_e is the number of electrons in the system. The density matrix D can be obtained by solving the KS equations (2) using standard linear algebra libraries, such as LAPACK[50] or Intel MKL.[51] An alternative route, which we follow in this work, is to use a density matrix purification scheme.[52,53] First, by computing the inverse square root of S,

$$S \mapsto S^{-\frac{1}{2}} \tag{4}$$

we can write the Hamiltonian in an orthonormal basis

$$H \mapsto \tilde{H} \equiv S^{-\frac{1}{2}} H S^{-\frac{1}{2}}. \tag{5}$$

and re-express (2) as a standard eigenvalue problem $\tilde{H}|\tilde{\phi}_\alpha\rangle = e_\alpha|\tilde{\phi}_\alpha\rangle$, where $|\tilde{\phi}_\alpha\rangle \equiv S^{1/2}|\phi_\alpha\rangle$. Next, we compute the density matrix $\tilde{D}$

$$\tilde{H} \to \tilde{D} \equiv \theta(\mu I - \tilde{H}) = \sum_{\alpha=1}^{N_e} \theta(\mu - e_\alpha)|\tilde{\phi}_\alpha\rangle\langle\tilde{\phi}_\alpha| \tag{6}$$

and finally re-express it in the original basis

$$\tilde{D} \mapsto D \equiv S^{-\frac{1}{2}} \tilde{D} S^{-\frac{1}{2}}. \tag{7}$$

The transformation in eq 6 is obtained using a standard density matrix purification scheme that is suitable for TPUs, namely the hole-particle canonical purification scheme,[52] which we elaborate on later in the paper.

If no further modifications are made (e.g., density matrix truncations in linear-scaling DFT), then the cost of computing D, whether by solving eq 2 or performing the four matrix transformations in eqs 4-7, scales as $O(N^3)$. This constitutes what is known as the *cubic wall* of DFT.

The density matrix D is used to derive several important quantities. The real-space electron density $n(\mathbf{r})$ is given by

$$n(\mathbf{r}) = \sum_{i,j}^{N} \chi_i(\mathbf{r}) D_{ij} \chi_j(\mathbf{r}) \tag{8}$$

which can be computed on a real-space grid.[46] The sum of occupied KS eigenvalues, given by $\mathrm{Tr}(H\,D) = \mathrm{Tr}(\tilde{H}\,\tilde{D})$, is also used to compute the total ground-state energy. Additionally, the *energy weighted density matrix* Q

$$Q = D\,H\,D \tag{9}$$

is also useful to compute atomic forces analytically.[46]

RESULTS

DFT with TPUs. The main result of our work is the successful use of TPUs to perform the four matrix transformations 4-7, thereby tackling the $O(N^3)$ computational bottleneck of DFT. We employed TPUs of the third generation, denoted v3. A single TPU v3 core contains two matrix multiply units (MXUs) to formidably accelerate matrix−matrix multiplication (matmul), resulting in about 10 teraFLOPS (floating point operations per second) of measured single-core matmul performance in single precision. Importantly for our purposes, matmuls are also available in double precision using a software-emulated 57-bit floating point format. In this approach, utilized algorithms require many more single precision floating point operations when operating in our emulated double precision than in single precision, and as a result, matmuls in double precision take ∼11× longer than in single precision.

The smallest available TPU configuration consists of 8 TPU v3 cores with a total of 128 GB of dedicated high bandwidth memory (HBM), controlled by a single host with 48 CPU cores. The largest configuration is a pod with 2048 TPU v3 cores and 32 TB of HBM, controlled by 256 hosts. Given a choice of configuration, the available TPU cores are directly connected to nearest neighbors in a 2D torus network through fast intercore interconnects (ICIs), see Figure 2. The ICIs are critical to maintaining high performance when distributing matmuls and other dense linear algebra operations over all available TPU cores. In this work, we used the JAX library[21−23] to write *single program multiple data* (SPMD) code and executed it on configurations made of p TPU cores, denoted v3-p, for p = 8, 32, 128, and 512.

The TPU hardware architecture is especially suited for dense large-scale matmuls, which we perform in distributed form using the SUMMA algorithm,[54] as recently demonstrated in ref 33. Here, it was shown that for sufficiently large matrices a v3-512 TPU can perform dense matmuls at near-optimal efficiency: the performance per TPU core (measured in single-precision FLOPS) is maintained at roughly 93% of the single TPU core maximum performance.[33] It is important to emphasize that TPUs are often ill-suited for other tasks, and hence the algorithms utilized in this work and those in ref 33 had to be picked carefully and may differ from more conventional choices used in CPUs or GPUs. The use of DM purification algorithms, rather than direct diagonalization, is especially attractive for TPUs since all steps can be evaluated from a series of matmuls. Clearly, transformations 5 and 7 require large-scale matmuls. Transformations 4 and 6 are implemented by an iteration involving matrix polynomials of small degree, where each polynomial requires a short sequence of matrix additions and multiplications. Specifically, the matrix inverse square root in 4 is implemented using a standard Newton-Schulz iteration,[55] whereas for the density matrix purification in 6, we implemented the hole-particle canonical purification scheme.[52] Further algorithm details can be found in the Supporting Information.

For benchmarking purposes, we have performed end-to-end DFT computations on a sequence of increasingly large water clusters with geometries obtained from standard molecular dynamics simulations (see the Supporting Information). We leverage the DFT code FHI-aims[46,47] to set up and drive calculations using CPUs and then use the TPUs to tackle the $O(N^3)$ dense linear algebra bottlenecks 4-7. We also utilize the *ELectronic Structure Infrastructure* (ELSI) library[48,49] to facilitate the integration of FHI-aims and the TPU solver. In particular, the DFT Hamiltonian build time and associated computational scaling and parallelization are dictated exclusively by the FHI-aims code, which uses numeric atom-centered orbitals (NAOs) with an explicit finite spatial extent, and a truncated multipole expansion to accomplish low prefactor and efficient scaling of the Hamiltonian matrix build. While the computational time required to build the DFT Hamiltonian may vary greatly between different systems with the same total number of orbitals N (due to possible differences in the resulting sparsity in the systems), the computational time required for the $O(N^3)$ DM purification step performed on the TPU has much less variability since dense matrix operations are assumed, which do not utilize any

https://doi.org/10.1021/acs.jctc.2c00876
J. Chem. Theory Comput. 2023, 19, 25−32

sparsity present (see the Supporting Information for more discussion). Thus, we emphasize that the TPU wall times, which are reported throughout only for water clusters, are fairly robust with respect to different systems with the same total number of orbitals.

Throughout this work, we perform all-electron calculations using the PBE exchange-correlation functional and utilize an NAO basis set such that each H_2O molecule contributes 10 electrons, represented by 24 orbitals (5 for each hydrogen atom and 14 for the oxygen atom). First we consider a single TPU board with 8 TPU v3 cores controlled by a host with 48 CPU cores, and we run FHI-aims on the host. Figure 3 shows

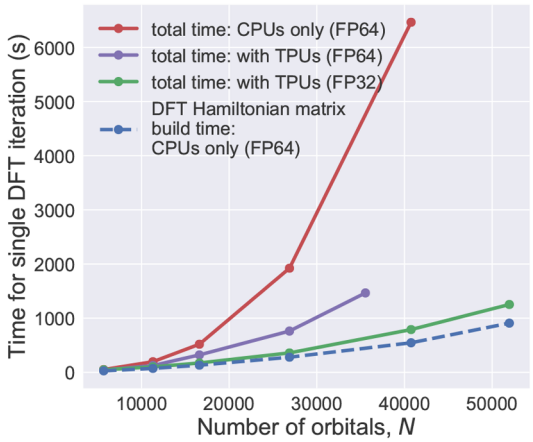

Figure 3. Wall times for a single DFT iteration on water clusters, using a TPU board composed of a CPU host (48 CPU cores) and 8 TPU cores with 128 GB of HBM. Green and purple curves correspond to using single and double precision in the TPU solver, respectively. The dashed blue curve corresponds to the CPU time spent on FHI-aims (always in double precision) and should be subtracted from the other curves in order to obtain the time spent on the TPU solvers. For reference, in red we also plot the time required for a CPU-only computation using the *eigenvalue soLvers for Petaflop Applications* (ELPA), a highly parallelized eigensolver library,[56,57] run on 48 CPU cores.

the wall time for a single DFT iteration (including both Hamiltonian build on CPUs and density matrix purification on TPUs) as a function of the size of the water cluster, which ranges from a few thousand to $N \approx 50\,000$ orbitals. When using the TPU solver in single precision (green curve), we see that the $O(N)$ Hamiltonian build on 48 CPU cores takes longer than the $O(N^3)$ density matrix purification run on 8 TPU cores, thus shifting the bottleneck. Using the TPU solver in double precision is an order of magnitude slower and saturates the TPU's HBM for $N \approx 36\,000$ orbitals.

Then we consider larger TPU configurations, of up to 512 TPU v3 cores, to perform end-to-end DFT computations on larger clusters, of up to 10 327 water molecules (or $N = 247\,848$ orbitals). Figure 1 shows the TPU wall time for the $O(N^3)$ density matrix purification for one DFT iteration. These include 350 (5 434) seconds for a density matrix purification in single (double) precision on the largest cluster, demonstrating feasibility of DFT computations at that scale of a quarter of a million orbitals.

Dynamic Precision on TPUs. In our implementation, early DFT iterations are treated with single precision, and later ones are treated with double precision. This *dynamic precision* approach allows us to cut down on the use of double precision matmuls on TPUs (which are significantly slower than single precision ones) without sacrificing accuracy of the final converged DFT result. Our criteria to switch precision is based on relative density changes, using the L^1 norm, defined as $L^1[f(\mathbf{r})] \equiv \int d^3r\, |f(\mathbf{r})|$, and relative energy changes

$$\frac{1}{N_e} L^1[n^{[i]}(\mathbf{r}) - n^{[i-1]}(\mathbf{r})] < \epsilon \quad \text{and} \tag{10}$$

$$|E^{[i]} - E^{[i-1]}|/|E^{[i]}| < \epsilon \tag{11}$$

where $n^{[i]}(\mathbf{r})$ is the real-space density at DFT iteration i, and $E^{[i]}$ is the corresponding total ground-state energy, and we use $\epsilon = 5 \times 10^{-7}$ for single precision.

Figure 4 shows the convergence trajectory of a dynamic precision DFT calculation for the largest cluster we have

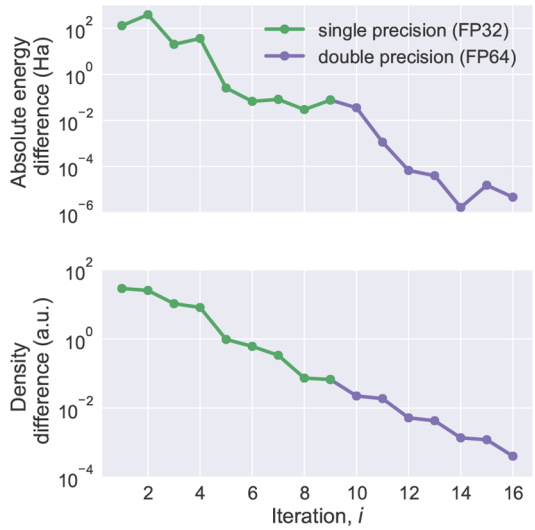

Figure 4. Convergence trajectory of an end-to-end dynamic precision DFT calculation on a $(H_2O)_{10327}$ cluster. The absolute total energy differences between subsequent DFT iterations, i and $i - 1$, are plotted (top). The corresponding difference in real-space densities within the L^1 norm is plotted (bottom).

considered. We are able to converge such a DFT calculation to a fairly tight convergence threshold using first 9 single precision DFT iterations, followed by 7 double precision DFT iterations. In a smaller cluster, $(H_2O)_{1481}$ with $N = 35\,544$ orbitals, a smaller number of double precision iterations are required for convergence, resulting in an overall DFT calculation time that is under 5 h on a single TPU board (v3−8), see the Supporting Information.

DISCUSSION

This work has successfully demonstrated that TPUs can both *accelerate* and *scale up* DFT computations. Significant *acceleration* is already achieved using only a single TPU board with 8 TPU v3 cores, see Figure 3. For instance, an end-to-end dynamic precision DFT computation with $N = 35\,544$ orbitals consisting of 12 iterations in single precision and 4 iterations in double precision yields converged results in under 5 h. For context, using double precision only and the highly optimized ELPA $O(N^3)$ solver with 48 CPUs, the same water cluster calculation required 20 h to achieve 16 DFT iterations.

In order to *scale up* the size of DFT computations while retaining high performance, two main ingredients are involved:

https://doi.org/10.1021/acs.jctc.2c00876
J. Chem. Theory Comput. 2023, 19, 25−32

(i) a larger amount of high bandwidth memory, scaling as $O(N^2)$, to be able to store dense $N \times N$ matrices, and (ii) a larger number of cores, with state-of-the-art intercore connectivity, to more effectively execute the $O(N^3)$ floating point operations involved in the required distributed matrix transformations. As shown in Figure 1, by using a number of cores that scales as $O(N^2)$ and commensurate amounts of HBM, we can scale up to N = 500 000 orbitals with wall times that only grow proportional to N.

Once the main ingredients (i) and (ii) are satisfied, the Input/Output (IO) time, i.e. the end-to-end communication time between the TPU and CPU, can become an important (and possibly limiting) factor. This IO step is not exclusive to TPUs, for instance, it is also relevant and analogous in GPU setups that require communication with CPUs. This step is parallelizable, such that by using a number of TPU and CPU cores that scale as $O(N^2)$, the total IO time remains constant $O(1)$. However, in this context, obtaining such optimality will depend on specific implementation details of the DFT code utilized, such as the matrix distribution pattern on the CPU processor grid. Our current prototype implementation is modular and generalizeable, and IO times scale unfavorably as $O(N^2)$, even becoming the rate-limiting step in some cases (see the Supporting Information). Less general (but straightforward) engineering approaches are expected to be much more optimal but are beyond the scope of this work which aims to demonstrate the use of TPUs in a more general context.

We emphasize that other hardware accelerators, most notably GPUs, can also accelerate and scale up DFT computations in a similar manner as discussed above, and ref 58 recently presented a useful and positive development in this direction.

Modern distributed GPU configurations are expected to achieve similar performance to TPUs in this regard; however, a direct comparison is complicated by the highly diverse nature of distributed GPU configurations found in practice. On the Summit supercomputer configuration, it has been reported that 432 distributed Nvidia V100 GPUs can perform matmuls for dense N > 500 000 matrices with a performance per GPU (measured in FLOPS) that is roughly 85% of the single V100 GPU maximum performance.[59]

Here we have focused, for simplicity, on applying DFT to clusters of water molecules. More complicated systems may present additional difficulties. For instance, protein−ligand complexes often require more elaborate schemes, such as including solvation to facilitate the convergence of the DFT iteration.[60,61] Work in progress shows that our TPU-based large-scale DFT computations can also successfully address protein−ligand complexes with explicit solvents, as well as in a variety of other large systems, including DNA segments, carbon nanotubes, and graphene surfaces. In addition to single-point DFT energy calculations, analytical forces can also be extracted from the TPU-calculated *energy-weighted density matrix*, enabling large-scale geometry optimization or ab initio molecular dynamics calculations.

DFT is a highly successful quantum-based method, but it is ultimately a consistent-field approximation, which may not be accurate enough for certain applications. Fortunately, TPUs can also accelerate and scale up other, more accurate quantum chemistry approaches where the computational bottleneck is again given by dense linear algebra operations. For example, in density matrix renormalization group (DMRG)[62] calculations, TPUs can be used to reach an unprecedentedly large bond dimension D = 65 536.[35] Similarly, we anticipate that TPUs will thrive in other methods such as coupled cluster[63] and Moller−Plesset perturbation theory.[64] Even when applying such higher-level methods, large-scale DFT may still be a crucial piece in simulations that require a quantum-mechanically treated region that embeds a subsystem treated with higher-level correlated methods.[65]

To conclude, in this work we have successfully repurposed TPUs as quantum chemistry supercomputers by tackling the $O(N^3)$ computational bottleneck of density functional theory. We demonstrated performance and scalability with a water cluster with N = 247 848 orbitals, which to our knowledge is the largest $O(N^3)$ DFT computation to date. We remark that cloud-based TPUs, and other hardware accelerators such as GPUs, are more accessible and affordable than traditional supercomputer resources. Our work thus paves the way toward accessible and straightforward use of quantum chemistry computational methods for much larger systems than were previously possible.

■ ASSOCIATED CONTENT

Supporting Information

The Supporting Information is available free of charge at https://pubs.acs.org/doi/10.1021/acs.jctc.2c00876.

Orthogonalization details, purification details, FHI-AIMS TPU integration details, and dynamic precision on smaller water clusters (PDF)

■ AUTHOR INFORMATION

Corresponding Author

Ryan Pederson − *Department of Physics and Astronomy, University of California, Irvine, California 92617, United States; X, the Moonshot Factory, Mountain View, California 94043, United States; Sandbox@Alphabet, Mountain View, California 94043, United States;* orcid.org/0000-0002-7228-9478; Email: pedersor@uci.edu

Authors

John Kozlowski − *Department of Chemistry, University of California, Irvine, California 92617, United States; X, the Moonshot Factory, Mountain View, California 94043, United States; Sandbox@Alphabet, Mountain View, California 94043, United States;* orcid.org/0000-0003-1227-9291

Ruyi Song − *Department of Chemistry, Duke University, Durham, North Carolina 27708, United States; X, the Moonshot Factory, Mountain View, California 94043, United States; Sandbox@Alphabet, Mountain View, California 94043, United States;* orcid.org/0000-0002-0320-7803

Jackson Beall − *SandboxAQ, Palo Alto, California 94304, United States; Sandbox@Alphabet, Mountain View, California 94043, United States*

Martin Ganahl − *SandboxAQ, Palo Alto, California 94304, United States; Sandbox@Alphabet, Mountain View, California 94043, United States*

Markus Hauru − *The Alan Turing Institute, London NW1 2DB, England, U.K.; Sandbox@Alphabet, Mountain View, California 94043, United States*

Adam G. M. Lewis − *SandboxAQ, Palo Alto, California 94304, United States; Sandbox@Alphabet, Mountain View, California 94043, United States*

https://doi.org/10.1021/acs.jctc.2c00876
J. Chem. Theory Comput. 2023, 19, 25−32

Yi Yao − *Thomas Lord Department of Mechanical Engineering and Materials Science, Duke University, Durham, North Carolina 27708, United States*

Shrestha Basu Mallick − *X, the Moonshot Factory, Mountain View, California 94043, United States; Sandbox@Alphabet, Mountain View, California 94043, United States*

Volker Blum − *Department of Chemistry and Thomas Lord Department of Mechanical Engineering and Materials Science, Duke University, Durham, North Carolina 27708, United States;* orcid.org/0000-0001-8660-7230

Guifre Vidal − *X, the Moonshot Factory, Mountain View, California 94043, United States; Sandbox@Alphabet, Mountain View, California 94043, United States; Google Quantum AI, Mountain View, California 94043, United States*

Complete contact information is available at: https://pubs.acs.org/10.1021/acs.jctc.2c00876

Notes

The authors declare the following competing financial interest(s): V.B. received compensation as an advisor from Google during part of this work. V.B. is also a board member of MS1P e.V., the non-profit organization that licenses the FHI-aims electronic structure code used in this work. V.B. does not receive any financial gains from this position.

■ ACKNOWLEDGMENTS

The authors would like to thank Toru Shiozaki and Garnet Kin-Lic Chan for suggesting to investigate the use of TPUs to accelerate mean-field quantum chemistry methods (by accelerating matrix multiplications for a diagonalization-free construction of the density matrix, as in the density matrix purification used in this paper) and Toru Shiozaki, Garnet Kin-Lic Chan, Chase Roberts, and Stefan Leichenauer for previous exploratory work in this direction. Also, special thanks go to Xing Zhang and Garnet Kin-Lic Chan for work adjusting PySCF, as part of an ongoing integration of our TPU solver, to be described elsewhere, and to David Bowler, Tsuyoshi Miyazaki, and Jun-ichi Iwata for help in documenting the largest DFT computation run on the K computer. Fianlly, the authors would also like to thank Giuseppe M. J. Barca, Anudhyan Boral, Michael Brenner, Kieron Burke, Rafael Gomez-Bombarelli, J. W. Feng, Filipp Furche, Andreas Goeller, Stephan Hoyer, Olivier Lacombe, Stefan Leichenauer, Lin Lin, Ruben Martin Romo, Todd Martinez, Anders M. N. Niklasson, Nicholas Rubin, Zak Stone, Matthias Tan, Keiran Thompson, Edward Valeev, and Jae Yoo for useful discussions and comments. Research was supported with Cloud TPUs from Google's TPU Research Cloud (TRC). Sandbox is a team within the Alphabet family of companies, which includes Google, Verily, Waymo, X, and others. G.V. is a CIFAR fellow in the Quantum Information Science Program, a Distinguished Invited Professor at the Institute of Photonic Sciences (ICFO), and a Distinguished Visiting Research Chair at Perimeter Institute. Research at Perimeter Institute was supported by the Government of Canada through the Department of Innovation, Science and Economic Development and by the Province of Ontario through the Ministry of Research, Innovation, and Science. R.S. and Y.Y. were partially supported by the National Science Foundation (NSF), USA under Award No. 1450280.

■ REFERENCES

(1) Duan, D.; Yu, H.; Xie, H.; Cui, T. Ab initio approach and its impact on superconductivity. *Journal of Superconductivity and Novel Magnetism* **2019**, *32*, 53−60.

(2) Cavasotto, C. N; Adler, N.S; Aucar, M. G Quantum chemical approaches in structure-based virtual screening and lead optimization. *Frontiers in chemistry* **2018**, *6*, 188.

(3) Yu, J.; Xie, L.-H.; Li, J.-R.; Ma, Y.; Seminario, J. M; Balbuena, P. B CO2 capture and separations using MOFs: computational and experimental studies. *Chem. Rev.* **2017**, *117*, 9674−9754.

(4) Jones, G. O.; Yuen, A.; Wojtecki, R. J; Hedrick, J. L; Garcia, J. M Computational and experimental investigations of one-step conversion of poly (carbonate) s into value-added poly (aryl ether sulfone) s. *Proc. Natl. Acad. Sci. U. S. A.* **2016**, *113*, 7722−7726.

(5) Boschetto, G.; Xu, T.; Yehya, M.; Thireau, J.; Lacampagne, A.; Charlot, B., Gil, T.; Todri-Sanial, A.Exploring 1D and 2D nanomaterials for health monitoring wearable devices. In *2021 IEEE International Conference on Flexible and Printable Sensors and Systems (FLEPS)*; IEEE: 2021; pp 1−4, DOI: 10.1109/FLEPS51544.2021.9469864.

(6) Frost, J. M.; Butler, K. T.; Brivio, F.; Hendon, C. H.; Van Schilfgaarde, M.; Walsh, A. Atomistic origins of high-performance in hybrid halide perovskite solar cells. *Nano Lett.* **2014**, *14*, 2584−2590.

(7) Urban, A.; Seo, D.-H.; Ceder, G. Computational understanding of Li-ion batteries. *npj Computational Materials* **2016**, *2*, 16002.

(8) Jones, R. O. Density functional theory: Its origins, rise to prominence, and future. *Reviews of modern physics* **2015**, *87*, 897.

(9) Austin, B.Nersc-10 workload analysis (data from 2018). https://portal.nersc.gov/project/m888/nersc10/workload/N10_Workload_Analysis.latest.pdf (accessed 2022-11-20).

(10) Talirz, L.; Ghiringhelli, L. M.; Smit, B. Trends in Atomistic Simulation Software Usage. *Living Journal of Computational Molecular Science* **2021**, *3*, 1483.

(11) Huhn, W. P.; Lange, B.; Yu, V. W.-z.e; Yoon, M.; Blum, V. GPU acceleration of all-electron electronic structure theory using localized numeric atom-centered basis functions. *Comput. Phys. Commun.* **2020**, *254*, 107314.

(12) Seritan, S.; Bannwarth, C.; Fales, B. S.; Hohenstein, E. G.; Isborn, C. M.; Kokkila-Schumacher, S. I. L.; Li, X.; Liu, F.; Luehr, N.; Snyder, J. W., Jr.; Song, C.; Titov, A. V.; Ufimtsev, I. S.; Wang, L.-P.; Martínez, T. J. TeraChem: A graphical processing unit-accelerated electronic structure package for large-scale ab initio molecular dynamics. *WIREs Computational Molecular Science* **2021**, *11*, e1494.

(13) Aprà, E.; Bylaska, E. J.; de Jong, W. A.; Govind, N.; Kowalski, K.; Straatsma, T. P.; Valiev, M.; van Dam, H. J. J.; Alexeev, Y.; Anchell, J.; Anisimov, V.; Aquino, F. W.; Atta-Fynn, R.; Autschbach, J.; Bauman, N. P.; Becca, J. C.; Bernholdt, D. E.; Bhaskaran-Nair, K.; Bogatko, S.; Borowski, P.; Boschen, J.; Brabec, J.; Bruner, A.; Cauët, E.; Chen, Y.; Chuev, G. N.; Cramer, C. J.; Daily, J.; Deegan, M. J. O.; Dunning, T. H.; Dupuis, M.; Dyall, K. G.; Fann, G. I.; Fischer, S. A.; Fonari, A.; et al. NWChem: Past, present, and future. *J. Chem. Phys.* **2020**, *152*, 184102.

(14) Frisch, M. J.; Trucks, G. W.; Schlegel, H. B.; Scuseria, G. E.; Robb, M. A.; Cheeseman, J. R.; Scalmani, G.; Barone, V.; Petersson, G. A.; Nakatsuji, H.; Li, X.; Caricato, M.; Marenich, A. V.; Bloino, J.; Janesko, B. G.; Gomperts, R.; Mennucci, B.; Hratchian, H. P.; Ortiz, J. V.; Izmaylov, A. F.; Sonnenberg, J. L.; Williams- Young, D.; Ding, F.; Lipparini, F.; Egidi, F.; Goings, J.; Peng, B.; Petrone, A.; Henderson, T.; Ranasinghe, D.; Zakrzewski, V. G.; Gao, J.; Rega, N.; Zheng, G.; Liang, W.; Hada, M.; Ehara, M., Toyota, K.; Fukuda, R.; Hasegawa, J.; Ishida, M.; Nakajima, T.; Honda, Y.; Kitao, O.; Nakai, H.; Vreven, T.; Throssell, K.; Montgomery, J. A., Jr.; Brothers, J. E.; Kudin, K. N.; Staroverov, V. N.; Keith, T. A.; Kobayashi, R.; Normand, J.; Raghavachari, K.; Rendell, A. P.; Burant, J. C.; Iyengar, S. S.; Tomasi, J.; Cossi, M.; Millam, J. M.; Klene, M.; Adamo, C.; Cammi, R.; Ochterski, J. W.; Martin, R. L.; Morokuma, K.; Farkas, O.; Foresman, J. B.; Fox, D. J.*Gaussian 16*, Revision C.01; Gaussian Inc.: Wallingford, CT, 2016.

(15) Gonze, X.; Jollet, F.; Abreu Araujo, F.; Adams, D.; Amadon, B.; Applencourt, T.; Audouze, C.; Beuken, J.-M.; Bieder, J.; Bokhanchuk, A.; Bousquet, E.; Bruneval, F.; Caliste, D.; Côté, M.; Dahm, F.; Da Pieve, F.; Delaveau, M.; Di Gennaro, M.; Dorado, B.; Espejo, C.; Geneste, G.; Genovese, L.; Gerossier, A.; Giantomassi, M.; Gillet, Y.; Hamann, D. R.; He, L.; Jomard, G.; Laflamme Janssen, J.; Le Roux, S.; Levitt, A.; Lherbier, A.; Liu, F.; Lukačević, I.; Martin, A.; et al. Recent developments in the ABINIT software package. *Comput. Phys. Commun.* **2016**, *205*, 106−131.
(16) Genovese, L.; Videau, B.; Ospici, M.; Deutsch, T.; Goedecker, S.; Méhaut, J.-F. Daubechies wavelets for high performance electronic structure calculations: The BigDFT project. *Comptes Rendus Mécanique* **2011**, *339*, 149−164.
(17) Hacene, M.; Anciaux-Sedrakian, A.; Rozanska, X.; Klahr, D.; Guignon, T.; Fleurat-Lessard, P. Accelerating VASP electronic structure calculations using graphic processing units. *Journal of computational chemistry* **2012**, *33*, 2581−2589.
(18) Wu, H. B.; Lou, X. W. D. Metal-organic frameworks and their derived materials for electrochemical energy storage and conversion: Promises and challenges. *Science Advances* **2017**, *3*, eaap9252.
(19) Jouppi, N.; Yoon, D.; Kurian, G.; Li, S.; Patil, N.; Laudon, J.; Young, C.; Patterson, D. A domain-specific supercomputer for training deep neural networks. *Communications of the ACM* **2020**, *63*, 67−78.
(20) Jouppi, N. P.; Young, C.; Patil, N.; Patterson, D.; Agrawal, G.; Bajwa, R.; Bates, S.; Bhatia, S.; Boden, N.; Borchers, A.; Boyle, R.; Cantin, P.-l.; Chao, C.; Clark, C.; Coriell, J.; Daley, M.; Dau, M.; Dean, J.; Gelb, B.; Ghaemmaghami, T. V.; Gottipati, R.; Gulland, W.; Hagmann, R.; Ho, C. R.; Hogberg, D.; Hu, J.; Hundt, R.; Hurt, D.; Ibarz, J.; Jaffey, A.; Jaworski, A.; Kaplan, A.; Khaitan, H.; Killebrew, D.; Koch, A.; Kumar, N.; Lacy, S.; Laudon, J.; Law, J.; Leary, C.; Diemthu, L.; Liu, Z.; Lucke, K.; Lundin, A.; MacKean, G.; Maggiore, A.; Mahony, M.; Miller, K.; Nagarajan, R.; Narayanaswami, R.; Ni, R.; Nix, K.; Norrie, T.; Omernick, M.; Penukonda, N.; Phelps, A.; Ross, J.; Ross, M.; Salek, A.; Samadiani, E.; Severn, C.; Sizikov, G.; Snelham, M.; Souter, J.; Steinberg, D.; Swing, A.; Tan, M.; Thorson, G.; Tian, Bo, Toma, H.; Tuttle, E.; Vasudevan, V.; Walter, R.; Wang, W.; Wilcox, E.; Yoon, D. H.In-Datacenter Performance Analysis of a Tensor Processing Unit. In *Proceedings of the 44th Annual International Symposium on Computer Architecture ISCA'17*; Association for Computing Machinery: New York, NY, USA, 2017; pp 1−12, DOI: 10.1145/3079856.3080246.
(21) Bradbury, J.; Frostig, R.; Hawkins, P.; Johnson, M. J.; Leary, C.; Maclaurin, D.; Necula, G.; Paszke, A.; VanderPlas, J.; Wanderman-Milne, S.; Zhang, Q.*JAX: composable transformations of Python +NumPy programs*; 2018.
(22) Frostig, R.; Johnson, M.; Leary, C.*Compiling machine learning programs via high-level tracing*; 2018.
(23) Abadi, M.; Barham, P.; Chen, J.; Chen, Z.; Davis, A.; Dean, J.; Devin, M.; Ghemawat, S.; Irving, G.; Isard, M.; Kudlur, M.; Levenberg, J.; Monga, R.; Moore, S.; Murray, D. G.; Steiner, B.; Tucker, P.; Vasudevan, V.; Wicke, M.; Warden, P.; Yu, Y.; Zheng, X.et al.TensorFlow: A System for Large-Scale Machine Learning. In *Proceedings of the 12th USENIX Conference on Operating Systems Design and Implementation, OSDI'16*; USENIX Association: USA, 2016; pp 265−283.
(24) Belletti, F.; King, D.; Yang, K.; Nelet, R.; Shafi, Y.; Shen, Y.-F.; Anderson, J.Tensor processing units for financial Monte Carlo. In *Proceedings of the 2020 SIAM Conference on Parallel Processing for Scientific Computing*; 2020; pp 12−23, DOI: 10.1137/1.9781611976137.2.
(25) Wang, Q.; Ihme, M.; Chen, Y.-F.; Anderson, J. A tensorflow simulation framework for scientific computing of fluid flows on tensor processing units. *Comput. Phys. Commun.* **2022**, *274*, 108292.
(26) Pan, Z.; Mishra, P.Hardware acceleration of explainable machine learning using tensor processing units. 2021, arXiv:2103.11927. *arXiv preprint*. https://arxiv.org/abs/2103.11927 (accessed 2022-12-08).
(27) Lu, T.; Marin, T.; Zhuo, Y.; Chen, Y.-F.; Ma, C.Accelerating MRI reconstruction on TPUs. In *2020 IEEE High Performance Extreme Computing Conference (HPEC)*; IEEE: 2020; pp 1−9, DOI: 10.1109/HPEC43674.2020.9286192.
(28) Lu, T.; Marin, T.; Zhuo, Y.; Chen, Y.-F.; Ma, C.Nonuniform fast Fourier transform on TPUs. In *2021 IEEE 18th International Symposium on Biomedical Imaging (ISBI)*; IEEE: 2021; pp 783−787, DOI: 10.1109/ISBI48211.2021.9434068.
(29) Lu, T.; Chen, Y.-F.; Hechtman, B.; Wang, T.; Anderson, J. Large-scale discrete Fourier transform on TPUs. *IEEE Access* **2021**, *9*, 93422−93432.
(30) Huot, F.; Chen, Y.-F.; Clapp, R.; Boneti, C.; Anderson, J.High-resolution imaging on TPUs. 2019, arXiv:1912.08063. *arXiv preprint*. https://arxiv.org/abs/1912.08063 (accessed 2022-12-08).
(31) Morningstar, A.; Hauru, M.; Beall, J.; Ganahl, M.; Lewis, A. GM; Khemani, V.; Vidal, G. Simulation of quantum many-body dynamics with Tensor Processing Units: Floquet prethermalization. *PRX Quantum* **2022**, *3*, 020331.
(32) Hauru, M.; Morningstar, A.; Beall, J.; Ganahl, M.; Lewis, A.; Vidal, G.Simulation of quantum physics with Tensor Processing Units: brute-force computation of ground states and time evolution. 2021, arXiv:2111.10466. *arXiv preprint*. https://arxiv.org/abs/2111.10466 (accessed 2022-12-08).
(33) Lewis, A. G. M.; Beall, J.; Ganahl, M.; Hauru, M.; Mallick, S. B.; Vidal, G. Large-scale distributed linear algebra with tensor processing units. *Proc. Natl. Acad. Sci. U. S. A.* **2022**, *119*, e2122762119.
(34) Gustafson, E.; Holzman, B.; Kowalkowski, J.; Lamm, H.; Li, A. Y.; Perdue, G.; Isakov, S. V.; Martin, O.; Thomson, R., Beall, J.; Ganahl, M.; Vidal, G.; Peters, E.Large scale multi-node simulations of Z2 gauge theory quantum circuits using Google Cloud Platform. In *2021 IEEE/ACM Second International Workshop on Quantum Computing Software (QCS)*; IEEE Computer Society: Los Alamitos, CA, USA, 2021; pp 72−79, DOI: 10.1109/QCS54837.2021.00012.
(35) Ganahl, M.; Beall, J.; Hauru, M.; Lewis, G. M. A.; Jae Hyeon Yoo, Y.; Zou, G.*Density Matrix Renormalization Group with Tensor Processing Units*. 2022, arXiv:2204.05693. arXiv preprint. https://arxiv.org/pdf/2204.05693.pdf (accessed 2022-12-08).
(36) Hohenberg, P.; Kohn, W. Inhomogeneous electron gas. *Physical review* **1964**, *136*, B864.
(37) Kohn, W.; Sham, L. J. Self-consistent equations including exchange and correlation effects. *Physical review* **1965**, *140*, A1133.
(38) Seidl, A.; Görling, A.; Vogl, P.; Majewski, J. A; Levy, M. Generalized Kohn-Sham schemes and the band-gap problem. *Phys. Rev. B* **1996**, *53*, 3764.
(39) Hasegawa, Y.; Iwata, J.-I.; Tsuji, M.; Takahashi, D.; Oshiyama, A.; Minami, K.; Boku, T.; Inoue, H.; Kitazawa, Y.; Miyoshi, I.; Yokokawa, M. Performance Evaluation of Ultra-Large-Scale First-Principles Electronic Structure Calculation Code on the K Computer. *Int. J. High Perform. Comput. Appl.* **2014**, *28*, 335−355.
(40) Prentice, J. C. A.; Aarons, J.; Womack, J. C.; Allen, A. E. A.; Andrinopoulos, L.; Anton, L.; Bell, R. A.; Bhandari, A.; Bramley, G. A.; Charlton, R. J.; Clements, R. J.; Cole, D. J.; Constantinescu, G.; Corsetti, F.; Dubois, S. M.-M.; Duff, K. K. B.; Escartín, J. M.; Greco, A.; Hill, Q.; Lee, L. P.; Linscott, E.; O'Regan, D. D.; Phipps, M. J. S.; Ratcliff, L. E.; Serrano, Á. R.; Tait, E. W.; Teobaldi, G.; Valerio, V.; Yeung, N.; Zuehlsdorff, T. J.; Dziedzic, J.; Haynes, P. D.; Hine, N. D. M.; Mostofi, A. A.; Payne, M. C.; Skylaris, C.-K.; et al. The ONETEP linear-scaling density functional theory program. *J. Chem. Phys.* **2020**, *152*, 174111.
(41) Bowler, D. R.; Miyazaki, T. Calculations for millions of atoms with density functional theory: linear scaling shows its potential. *J. Phys.: Condens. Matter* **2010**, *22*, 074207.
(42) Soler, J. M.; Artacho, E.; Gale, J. D; García, A.; Junquera, J.; Ordejón, P. The SIESTA method for ab initio order-N materials simulation. *J. Phys.: Condens. Matter* **2002**, *14*, 2745.
(43) VandeVondele, J.; Krack, M.; Mohamed, F.; Parrinello, M.; Chassaing, T.; Hutter, J. Quickstep: Fast and accurate density functional calculations using a mixed Gaussian and plane waves approach. *Comput. Phys. Commun.* **2005**, *167*, 103−128.

(44) Cole, D. J.; Skylaris, C.-K.; Rajendra, E.; Venkitaraman, A. R.; Payne, M. C. Protein-protein interactions from linear-scaling first-principles quantum-mechanical calculations. *Europhys. Lett.* **2010**, *91*, 37004.
(45) White, C. A; Johnson, B. G; Gill, P. MW; Head-Gordon, M. Linear scaling density functional calculations via the continuous fast multipole method. *Chem. Phys. Lett.* **1996**, *253*, 268−278.
(46) Blum, V.; Gehrke, R.; Hanke, F.; Havu, P.; Havu, V.; Ren, X.; Reuter, K.; Scheffler, M. Ab initio molecular simulations with numeric atom-centered orbitals. *Comput. Phys. Commun.* **2009**, *180*, 2175−2196.
(47) Blum, V.; Kokott, S.; Rossi, M.; Scheffler, M.FHI-AIMS. https://fhi-aims.org/ (accessed 2022-11-20).
(48) Yu, V. W.-z.; Campos, C.; Dawson, W.; García, A.; Havu, V.; Hourahine, B.; Huhn, W. P.; Jacquelin, M.; Jia, W.; Keçeli, M.; Laasner, R.; Li, Y.; Lin, L.; Lu, J.; Moussa, J.; Roman, J. E.; Vázquez-Mayagoitia, Á.; Yang, C.; Blum, V. Elsi — an open infrastructure for electronic structure solvers. *Comput. Phys. Commun.* **2020**, *256*, 107459.
(49) Yu, V. W.-z.; Corsetti, F.; García, A.; Huhn, W. P.; Jacquelin, M.; Jia, W.; Lange, B.; Lin, L.; Lu, J.; Mi, W.; Seifitokaldani, A.; Vázquez-Mayagoitia, Á.; Yang, C.; Yang, H.; Blum, V. Elsi: A unified software interface for Kohn-Sham electronic structure solvers. *Comput. Phys. Commun.* **2018**, *222*, 267−285.
(50) Anderson, E.; Bai, Z.; Bischof, C.; Blackford, S.; Demmel, J.; Dongarra, J.; Du Croz, J.; Greenbaum, A.; Hammarling, S.; McKenney, A.; Sorensen, D.*LAPACK Users' Guide*, 3rd ed.; Society for Industrial and Applied Mathematics: Philadelphia, PA, 1999.
(51) *Intel Math Kernel Library*; Intel Corporation: Santa Clara, USA, 2009; iSBN 630813-054US.
(52) Truflandier, L. A.; Dianzinga, R. M.; Bowler, D. R. Communication: Generalized canonical purification for density matrix minimization. *J. Chem. Phys.* **2016**, *144*, 091102.
(53) Kim, J.; Jung, Y. A perspective on the density matrix purification for linear scaling electronic structure calculations. *Int. J. Quantum Chem.* **2015**, *115*, 1141.
(54) Van De Geijn, R. A.; Watts, J. SUMMA: scalable universal matrix multiplication algorithm. *Concurrency: Practice and Experience* **1997**, *9*, 255−274.
(55) Higham, N. J. Stable iterations for the matrix square root. *Numerical Algorithms* **1997**, *15*, 227−242.
(56) Ků s, P.; Marek, A.; Köcher, S. S.; Kowalski, H.-H.; Carbogno, C.; Scheurer, Ch.; Reuter, K.; Scheffler, M.; Lederer, H. Optimizations of the eigensolvers in the elpa library. *Parallel Computing* **2019**, *85*, 167−177.
(57) Marek, A.; Blum, V.; Johanni, R.; Havu, V.; Lang, B.; Auckenthaler, T.; Heinecke, A.; Bungartz, H.-J.; Lederer, H. The ELPA library: scalable parallel eigenvalue solutions for electronic structure theory and computational science. *J. Phys.: Condens. Matter* **2014**, *26*, 213201.
(58) Das, S.; Motamarri, P.; Subramanian, V.; Rogers, D. M; Gavini, V. Dft-fe 1.0: A massively parallel hybrid CPU-GPU density functional theory code using finite-element discretization. *Computer Physics Communications* **2022**, *280*, 108473.
(59) Herault, T.; Robert, Y.; Bosilca, G.; Dongarra, J.Generic matrix multiplication for multi-gpu accelerated distributed-memory platforms over parsec. In *2019 IEEE/ACM 10th Workshop on Latest Advances in Scalable Algorithms for Large-Scale Systems (ScalA)*; IEEE: 2019; pp 33−41, DOI: 10.1109/ScalA49573.2019.00010.
(60) Lever, G.; Cole, D.l J; Hine, N. D. M.; Haynes, P. D; Payne, M. C Electrostatic considerations affecting the calculated homo-lumo gap in protein molecules. *J. Phys.: Condens. Matter* **2013**, *25*, 152101.
(61) Rudberg, E. Difficulties in applying pure Kohn−Sham density functional theory electronic structure methods to protein molecules. *J. Phys.: Condens. Matter* **2012**, *24*, 072202.
(62) White, S. R. Density matrix formulation for quantum renormalization groups. *Phys. Rev. Lett.* **1992**, *69*, 2863−2866.
(63) Fales, B S.; Curtis, E. R; Johnson, K G.; Lahana, D.; Seritan, S.; Wang, Y.; Weir, H.; Martínez, T. J.; Hohenstein, E. G. Performance of coupled-cluster singles and doubles on modern stream processing architectures. *J. Chem. Theory Comput.* **2020**, *16*, 4021−4028.
(64) Vogt, L.; Olivares-Amaya, R.; Kermes, S.; Shao, Y.; Amador-Bedolla, C.; Aspuru-Guzik, A. Accelerating resolution-of-the-identity second-order Møller-Plesset quantum chemistry calculations with graphical processing units. *J. Phys. Chem. A* **2008**, *112*, 2049−2057.
(65) Sun, Q.; Chan, G. K.-L. Quantum embedding theories. *Accounts of chemical research* **2016**, *49*, 2705−2712.

https://doi.org/10.1021/acs.jctc.2c00876
J. Chem. Theory Comput. 2023, 19, 25−32